# Off-axis electron holography and microstructure of $Ba_{0.5}Sr_{0.5}TiO_3$ thin films on $LaAlO_3$

H. F. Tian,[1] H. C. Yu,[1] X. H. Zhu,[2] Y. G. Wang,[1] D. N. Zheng,[2] H. X. Yang,[1] and J. Q. Li[1,*]
[1]*Beijing Laboratory of Electron Microscopy, Institute of Physics, Chinese Academy of Sciences, Beijing, 100080, China*
[2]*National Laboratory for Superconductivity, Institute of Physics, Chinese Academy of Sciences, Beijing, 100080, China*
(Received 30 September 2004; revised manuscript received 23 November 2004; published 17 March 2005)

Epitaxial $Ba_{0.5}Sr_{0.5}TiO_3$ thin films grown on the (001) $LaAlO_3$ substrates with a ferroelectric transition at about 250 K have been investigated by TEM and off-axis electron holography. Cross-sectional TEM observations show that the 350-nm-thick $Ba_{0.5}Sr_{0.5}TiO_3$ film has a sharp interface with notable misfit dislocations. Off-axis electron holographic measurements reveal that, at low temperatures, the ferroelectric polarization results in a remarkable positive potential on the interface and a negative potential on the film surface, and, at room temperature, certain charges could only accumulate at the interfacial dislocations and other defective areas.

DOI: 10.1103/PhysRevB.71.115419 PACS number(s): 61.14.Nm

Ferroelectric $(Ba_{1-x}Sr_x)$ $TiO_3$ thin films have recently become very attractive material due to their large dielectric constant $(\varepsilon_r)$ and high tunability $(\varepsilon_r)$ in semiconductor technology; the dielectric constant of this material can vary from a few hundreds to thousands by adjusting the Ba/Sr ratio, grain size, and temperature. Its Curie temperature decreases almost linearly with Sr content,[1] and the dielectric constant exhibits remarkable tunability under an applied dc electric field near the Curie temperature.[2–6] Moreover, by adjusting the Ba/Sr ratio, the film can be either a paraelectric or a ferroelectric semiconductor. Especially, when the ratio of $Ba/Sr \approx 1$, the $Ba_{0.5}Sr_{0.5}TiO_3/LaAlO_3$ film is in the paraelectric state with a good tunability at room temperature, and also presents the highest dielectric constant and the lowest loss of the tangent. These distinctive electric properties imply the potential applications of $(Ba_{1-x}Sr_x)$ $TiO_3$ thin films in the high-density dynamic random access memories, smart card memories, and tunable microwave devices.[2,3,7–10] High quality films, which can minimize the loss of the tangent, are requested for fabrication of the reliable and high performance devices. Because of the microstructure sensitivity of the $Ba_{1-x}Sr_xTiO_3$ films, detailed investigations of the microstructure and correlation to physical behaviors of the products are highly desirable for synthesis method evaluation and further application. Electron holography based on transmission electron microscopy (TEM) offers a promising way to understand and investigate ferroelectrics in the electron microscopy. In this paper, we report on the microstructure measured by cross-section TEM and electrostatic potential on defects, interface, and surface in $Ba_{0.5}Sr_{0.5}TiO_3/LaAlO_3$ (BST/LAO) identified by off-axis electron holography.

The BST thin films on (001) LAO substrate studied in the present work were prepared by pulsed laser deposition. Firstly, the BST films were grown under an oxygen pressure of about 25 Pa and at the temperature of 800°C to a thickness of about 200 nm in 10 min. Then, the films were post-annealed at 500°C under one atmosphere oxygen pressure for 30 min. Detailed depictions on the film growth and physical properties of the as-grown BST films were reported in Ref. 9. Electron microscopy and off-axis electron holography observations were carried out utilizing a Philips CM200/FEG transmission electron microscope equipped with the electrostatic biprism. Samples for cross-section TEM and electron holography investigations were prepared using a standard procedure consisting of gluing, cutting, mechanical polishing, dimpling, and ion milling. The holograms were acquired with a Gatan 794 multiscan charge-coupled device (CCD) camera, and processed using Gatan Digital Micrograph software including the "HOLOWORK" package. Off-axis electron holography provides information about the phase and amplitude of the exit electron wave after traversing through a specimen. This technique has been frequently applied to study ferroelectric materials[11–13] and was proved as one of the effective techniques in determining the characteristics of ferroelectrics.

Electron holography measurements in principle can provide the information on the distribution of electrostatic potential from surface to interface of the BST film due to charge accumulation. When the electron beams pass through a local electric field, interaction between the incident electron wave and the electrostatic potential within the specimen induces a local differential phase shift in the exit electron wave function. The phase shift directly proportional to the electrostatic potential distribution can be recorded in the hologram formed by interference of the perturbed exit electron wave function with the reference wave in vacuum, and the recorded electron hologram with high spatial resolution can provide information about the phase of the exit electron wave function via reconstruction of the interference pattern. The general relationship of the phase shift is $\varphi = \sigma \int V(x,y,z) d_Z$, where $V(x,y,z)$ is the potential distribution along the path of the incident electron passing through the specimen. For a heterostructure specimen, the projected potential contains two components: (1) the mean inner potential (MIP) of the material defined as a volume average of the electrostatic potential; and (2) the electrostatic potential caused by polarization fields. The mean inner potential is an essential property of a material; it usually has a value between 10 and 20 V. For the BST/LAO heterostructure, our experimental measurements suggest that, if the thickness of a probe area is well selected, the MIP difference between the film and substrate is so small that it only shows up as a

 

limited influence on the background in our reconstructured images. Considering the projected potential resulting from polarization effects, we assume that the BST films grow totally relaxed on the LAO substrates; spontaneous polarization yields notable changes of potential on the interface areas. The mesoscopic phase of the transmitted electron wave result from spontaneous polarization can be computed directly from the electric field $\vec{E}=-\vec{P}/\varepsilon$ induced by the polarization $\vec{P}$ in a material with dielectric constant $\varepsilon$, and the dielectric field is the derivative of the potential. So, $\varphi(x,y)=\sigma/\varepsilon\int\int\vec{P}d_Z\vec{d_r}$, the integral over $z$, can be interpreted as "projected polarization" $\vec{P}_{proj}=\int_{thickness}\vec{P}d_Z$.[11] Thus, we can obtain the correlations between the phase, electric field, potential, thickness, and polarization in the material. Generally, there are several factors that can contribute to a holographic phase shift across the heterostructure. However, if the sample is not strongly diffracting and has uniform potential through the thickness, the contrast in the phase image is proportional to the potential times the thickness. We can give the expression of the phase shift of the object as $\varphi(x,y)=C_E[V_0+V(x,y)]t(x,y)$, where $C_E$ is an energy-dependent constant which equals $7.295\times10^{-3}$ rad/(V nm) for the 200-KeV electron and $t$ is the thickness of the sample where electron waves are transmitted.

Experimental results from both TEM observations and x-ray diffraction (not shown) indicate that the $Ba_{0.5}Sr_{0.5}TiO_3$ film is epitaxially grown along the ⟨001⟩ direction on the (001) $LaAlO_3$ substrate. Figure 1(a) is a bright-field TEM image displaying the morphology of the as-grown film with a uniform thickness of about 350 nm. A remarkable feature of the film is the columnar structure with V-shaped grain boundaries as indicated with the solid lines; this structural feature is considered to arise from small relative rotations between the crystalline grains.[10] The presence of numerous steps and terraces on the film surface indicates different growing rates of the subgrains during film preparation. The well-defined epitaxial relationship between the film and substrate is illustrated by the corresponding electron-diffraction pattern present in Fig. 1(b). Two sets of electron-diffraction spots, arising, respectively, from the BST film and the LAO substrate, can be unambiguously indexed based on the $LaAlO_3$ structure (a cubic cell with the lattice parameter of 0.378 nm) and $Ba_{0.5}Sr_{0.5}TiO_3$ structure with the lattice constant of 0.394 nm. This pattern clearly exhibits the orientation relationship of $[010]_{BST}\|[010]_{LAO}$ and $[001]_{BST}\|[001]_{LAO}$. A lattice mismatch of ~4.2% between $Ba_{0.5}Sr_{0.5}TiO_3$ and $LaAlO_3$ can be obtained from splits of the diffraction spots. This lattice mismatch could result in distinctive dislocations on the interfacial area as discussed in the following context. The interface without reaction products between the film and substrate is clean and sharp as confirmed by the high-resolution TEM (HRTEM) image shown in Fig. 1(c), which shows the interface structure emphasizing the perfect quality of epitaxial growth and the sharp interface between the film and substrate. Figure 1(d) shows the TEM image with a large magnification from the square area in Fig. 1(c), in which the detailed interfacial atomic structure can be clearly recognized. Image

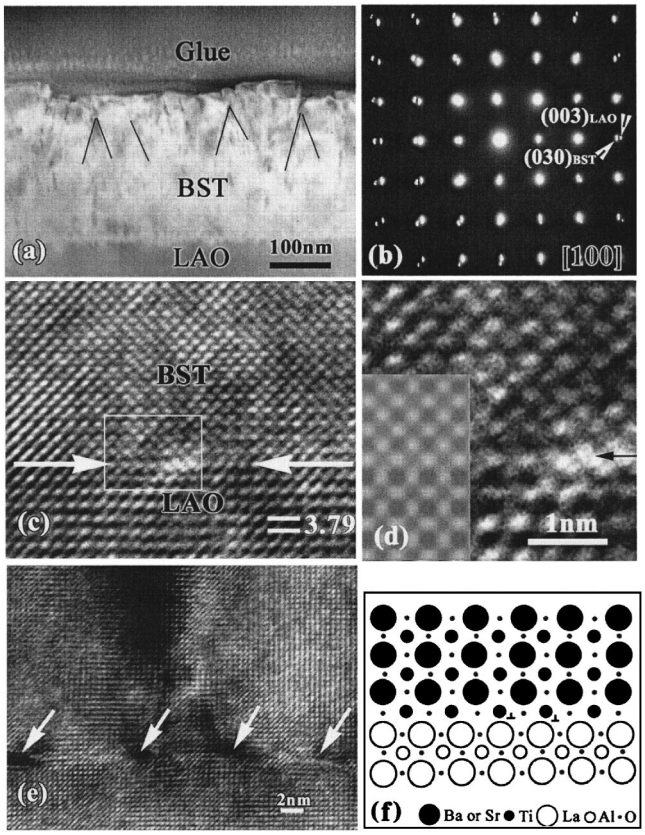


FIG. 1. (a) Bright-field TEM image showing morphology of the epitaxial BST film on LAO substrate. (b) Selected area electron-diffraction pattern from the interface area. (c) HRTEM image showing the details of the interface of epitaxial growth of BST film. (d) Large magnification TEM image with the theoretical simulation for the interface area. (e) HRTEM image showing the misfit dislocations on the interface. (f) Atomic structural model for an interfacial dislocation.

simulation based on the interface configuration of (BST)-(Ba,Sr)-$TiO_2$-/-LaO-(LAO) was performed for sample thickness ($t$) between 0.6 and 5 nm and a defocus value ($\Delta f$) between −10 and −60 nm; A theoretical image with $t=2.5$ nm and $\Delta f=-35$ nm is in good agreement with the experimental image as superposed on Fig. 1(d). Figure 1(e) displays a high-resolution TEM image showing the presence of numerous misfit dislocations on the interface. This dislocation array with a pseudoperiodicity of around $L=7.5$ nm is roughly coincident with theoretical prediction ($L_d=a_1a_2/(a_1-a_2)=19\times0.38$ nm$=7.2$ nm). Figure 1(f) schematically illustrates an atomic structural model with the characteristic of an edge-dislocation along the interface.

In order to determine the polarization of the BST film, we have performed a series of off-axis electron holography measurements at low temperatures. Below the Curie temperature of 250 K, the $Ba_{0.5}Sr_{0.5}TiO_3$ film transforms into a ferroelectric state, which results in charge redistributions due to ferroelectric polarization. For understanding the possible ferroelectric ordering as well as the spontaneous polarization, the potential distribution in the film has been measured at the temperature of 120 K by off-axis electron holography. Figure 2(a) shows a hologram taken at the surface of the film under

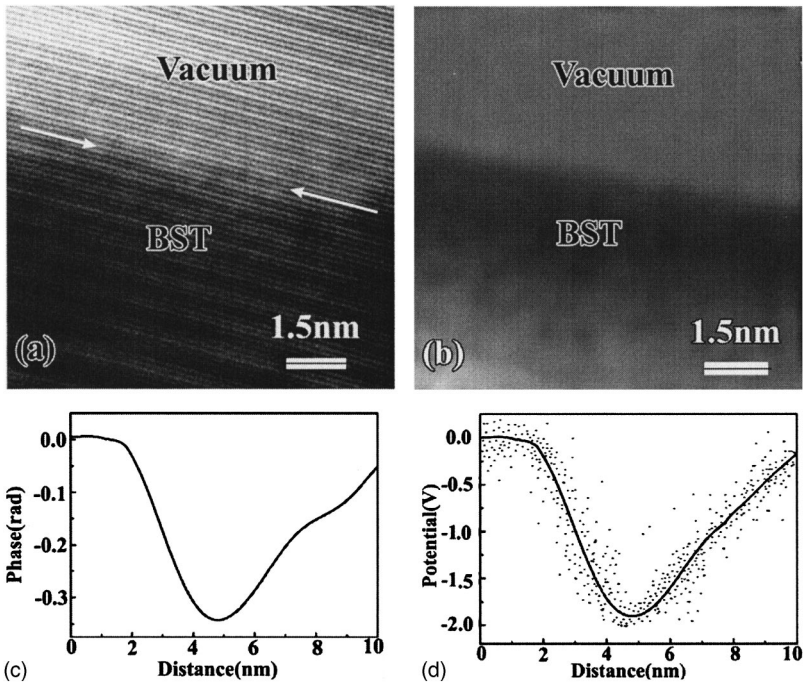


FIG. 2. (a) Hologram taken at 120 K for the surface of BST film. (b) Reconstructed phase change from obtained hologram. (c) Phase profile showing up a value at the position of film surface. (d) Potential variations from film to vacuum. The sample thickness was measured by convergent-beam electron diffraction.

a positive bias voltage of 90 V. The interference fringes with perfect visibility have an average space of ~0.16 nm, therefore, the spatial resolution in the reconstructed holograms, about three times of the fringe spacing, is better than 0.5 nm. The surface of the specimen yields a clear contrast as indicated by arrows. This hologram, in combination with the reference vacuum hologram, could give rise to a reconstructed phase image. Figure 2(b) shows the reconstructed phase image indicating the phase alternation from film to vacuum, permitting a more detailed analysis. The contrast in the vacuum phase is relatively lower than that in the film; a dark band appearing in the film surface indicates that the phase in this region is lower than that in the inner parts. Figure 2(c) illustrates a typical phase profile normal to the surface, showing that a vale appears at the surface position; Figure 2(d) shows the potential change from surface of the BST film to vacuum as a function of distance, which exhibits the potential profiles from numerous distinctive positions normalized by film thickness which is measured to be ~25 nm and assumed to be constant within a few nanometers. The potential change profile is in connection with the charge distribution through the Poisson equation. This result directly suggests that certain negative charges are accumulated on the film surface resulting in delay of the wave front of the exit electron wave function.

To get a thorough understanding of the spontaneous polarization process, an electron holography study was also performed on the interface. Figure 3(a) is a hologram taken at the interface region (indicated by arrows) without edge dislocations under a positive bias potential of 90 V. Because of the limited interference scope in our experiment, the hologram containing both the vacuum and the sample edge was taken separately for correction of the phase profile. A reference hologram without the sample was acquired for correction of holographic fringe distortions due to the spurious effects caused by the image system, the inhomogeneities contamination in the biprism wire, and the nonisoplanicity of the incident illumination.[14] The Hanning window, applying three orders, was used in reconstruction to reduce the edge effect and in compensation for the phase shift artificially produced by the Fresnel fringe from the filament electrode.[15] Although there is not much contrast change between the film and the substrate, certain weak contrast alternation inside the film is likely caused by the column structure. Figure 3(b) shows an averaged line scan from the substrate to the film in the reconstructed phase image showing a clear peak of the phase profile at the interface position (indicated by the arrow). Figure 3(c) illustrates the potential change normalized by the experimental specimen thickness of 30 nm which is consistent with Fig. 3(b). These data suggest that net positive charges appear locally at the interface resulting in leading of the wave front of the exit electron wave function. In combination with the experimental results obtained from the surface area, we can generally conclude that net charges with opposite signs accumulate, respectively, on the BST/LAO interface and BST surface, and a spontaneous polarization occurs along the ⟨001⟩ axis direction in the ferroelectric state. This kind of polarization, as reported in previous studies, is essentially in connection with the movements of Ba(Sr) and O atoms in opposite directions as schematically illustrated in Fig. 3(d).[11]

The misfit dislocations with unpaired dangling bonds could capture charges to form the localized electrostatic field along the dislocation lines, and therefore influence the dielectric properties of the film. Actually, room-temperature measurements of dielectric properties indicate that the $Ba_{0.5}Sr_{0.5}TiO_3$ films are in a paraelectric state and have the relative dielectric constant of $\varepsilon_r \sim 1200$, the loss tangent of 0.016, and the tunability of about 60%. On the other hand, careful analyses suggest that these kinds of films in general show a faintly ferroelectric property. Figure 4(a) shows a papilionaceous-shaped curve obtained under 1 MHz at

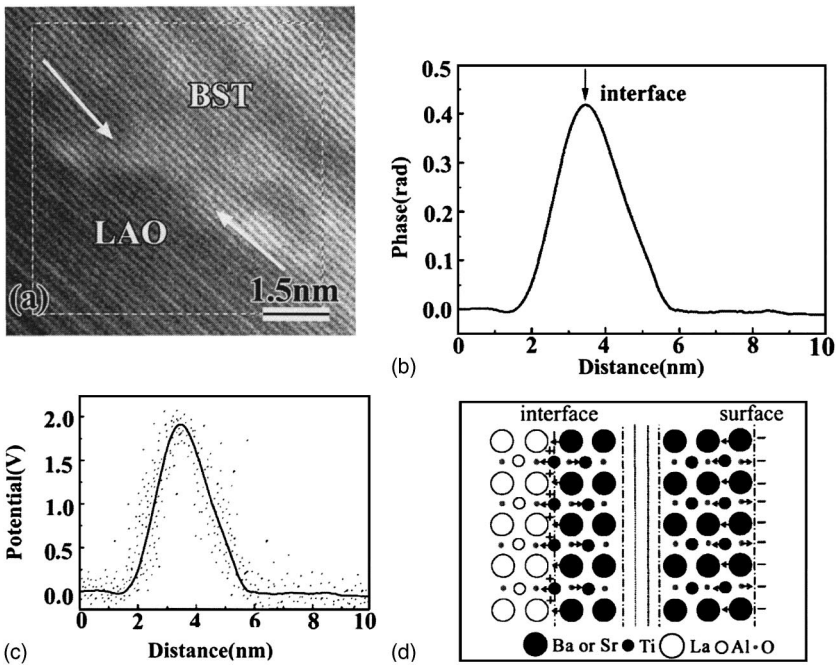


FIG. 3. (a) Hologram taken at 120 K for the interface area. (b) Phase profile showing a valley across the BST/LAO interface. (c) Potential change across the interface area. (d) Schematic model of atom movement in the film due to spontaneous polarization.

300 K. First, the capacitance-voltage ($C$-$V$) characteristics of the as-grown films were measured by using the interdigital capacitor technique with a HP4294A Precision LCR Meter. The capacitor consists of 50 fingers that are 1-mm long, 10-$\mu$m wide, and spaced 10-$\mu$m apart. The relative dielectric constant ($\varepsilon_r$) was extracted from the capacitance using the conformal mapping results of Gevorgian *et al.*[16] The presence of hysteresis in the $\varepsilon$-$v$ curve demonstrates the existence of local ferroelectric orders or interfacial space charges[5] in the $Ba_{0.5}Sr_{0.5}TiO_3$ film. Figure 4(b) shows a hologram taken from an area with clear interfacial dislocations by a positive bias of 120 V applied to the biprism. The lattice fringes superimposed on the fine holographic fringes show a typical interfacial dislocation (indicated by arrows). The reconstructed images were obtained using the primary sideband as mentioned in above context. Although there is no detectable phase change at the interface position as expected for the paraelectric state, a line scan across the misfit dislocation shows remarkable phase alternations. In order to improve the poor statistic of a single line scan, the averaged

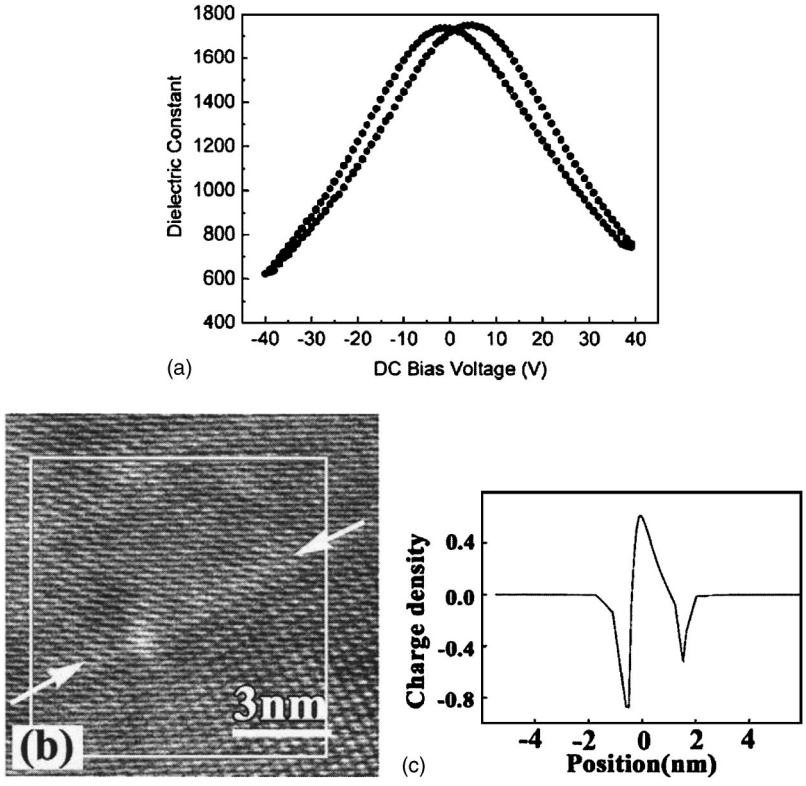


FIG. 4. (a) Dielectric constant as a function of applied dc bias voltage under 1 MHz at 300 K. (b) Electron hologram from an interface area with a notable misfit dislocation at 300 K. (c) Charge distributions cross this dislocation.

phase profile over 50 line scans taken in our analysis shows obviously a positive phase jump on the dislocation center. Differentiation of the phase profile as shown in Fig. 4(c) could predict the charge distribution around the dislocation, which demonstrates positive charges accumulating on the dislocation core with negative charges around. In accordance with the structural model [Fig. 1(d)] and our experimental results, this kind of charge distribution can be qualitatively understood as follows: The considerable stress on the misfit dislocations could either result in local oxygen vacancies or yields outward movements of oxygen ions so that net positive charges appear locally on the center area. In addition, our measurements also show that a small amount of charges accumulate on the intragrain boundaries at room temperature. These experimental results are consistent with the data of the dielectric measurements; the local charges and the related polarizations make the $\varepsilon$-$v$ curve papilionaceously shaped and give rise to the weak ferroelectric property in the room-temperature paraelectric state.

In conclusion, the $Ba_{0.5}Sr_{0.5}TiO_3$ thin films with ferroelectric transition at about 250 K, grown on the (001) $LaAlO_3$ substrates by pulsed laser deposition, have a well-defined epitaxial structure with a sharp interface and notable misfit dislocations. This kind of ferroelectric film has an evident ferroelectric polarization along the ⟨001⟩ direction at around 120 *K* as demonstrated by off-axis electron holographic investigations. As a result, positive and negative electric potentials, arising from charge accumulations, are directly detected on the interface and the film surface, respectively. Room-temperature measurements of electron holography reveal local positive charge accumulation on interfacial dislocations and some other grain boundaries in the $Ba_{0.5}Sr_{0.5}TiO_3$ thin film, which could result in weak ferroelectric properties as demonstrated by dielectric measurements.

We would like to thank Professor Y.Q. Zhou, Professor X.F. Duan, and Y. Li for their assistance in preparing samples. The work reported here was supported by the National Natural Science Foundation of China.

*Corresponding author. Email address: ljq@aphy.iphy.ac.cn

[1] Y. Gim, T. Hudson, Y. Fan, C. Kwon, A. T. Findikoglu, B. J. Gibbons, B. H. Park and Q. X. Jia, Appl. Phys. Lett. **77**, 1200 (2000).

[2] F. W. Van Keuls, R. R. Romanofsky, D. Y. Bohman, M. D. Winters, F. A. Miranda, C. H. Mueller, R. E. Treece, T. V. Rivkin, and D. Galt, Appl. Phys. Lett. **71**, 3075 (1997).

[3] K. R. Carroll, J. M. Pond, D. B. Chrisey, J. S. Horwitz, R. E. Leuchtner, and K. S. Grabowski, Appl. Phys. Lett. **62**, 1845 (1993).

[4] R. A. Chakalov, Z. G. Ivanov, Yu. A. Boikov, P. Larsson, E. Carlsson, S. Gevorgian, and T. Claeson, Physica C **308**, 279 (1998).

[5] H. C. Li, W. D. Si, A. D. West, and X. X. Xi, Appl. Phys. Lett. **73**, 190 (1998).

[6] I. Takeuchi, H. Chang, C. Gao, P. G. Schultz, X. D. Xiang, R. P. Sharma, M. J. Downes, and T. Venkatesan, Appl. Phys. Lett. **73**, 894 (1998).

[7] J. S. Scott, Ferroelectr. Rev. **1**, 1 (1998).

[8] A. T. Findikoglu, Q. X. Jia, I. H. Campbell, X. D. Wu, D. Reagor, C. B. Mombourquette, and D. McMurry, Appl. Phys. Lett. **66**, 3674 (1995).

[9] C. L. Chen, H. H. Feng, Z. Zhang, A. Brazdeikis, Z. J. Huang, W. K. Chu, C. W. Chu, F. A. Miranda, F. W. Van Leuls, R. R. Romanofsky, and Y. Liou, Appl. Phys. Lett. **75**, 412 (1999).

[10] H. J. Gao, C. L. Chen, B. Rafferty, S. J. Pennycook, G. P. Luo, and C. W. Chu, Appl. Phys. Lett. **75**, 2542 (1999).

[11] H. Lichte, M. Reibold, K. Brand, and M. Lehmann, Ultramicroscopy **93**, 199 (2002).

[12] X. Zhang, D. C. Joy, Y. Zhang, T. Hashimoto, L. Allard, and T. A. Nolan, Ultramicroscopy **51**, 21 (1993).

[13] W. Cao and C. Randall, Solid State Commun. **86**,435 (1993).

[14] M. R. McCartney, D. J. Smith, R. Hull, J. C. Bean, E. Voelkl, and B. Frost, Appl. Phys. Lett. **65**, 2603 (1994).

[15] K. Harada, M. Beleggia, J. Endo, H. Kasai, Y. Togawa, T. Matsuda, and A. Tonomura J. Electron Microsc. **52**, 369 (2003).

[16] S. Gevorgian, E. Carlsson, S. Rudner, L.-D. Wernlund, X. Wang, and U. Helwersson, IEE Proc., Part H: Microwaves, Antennas Propag. **143**, 397 (1996).